

Pyrazolato- and 3,5-Dimethylpyrazolato-Bridged Dinuclear Platinum(II), Palladium(II), and Their Mixed-Metal Complexes of 2,2'-Bipyrimidine. Syntheses, Structures, and Luminescent Properties

Keisuke Umakoshi,^{*1} Kazutoyo Kimura,¹ Yong Hun Kim,¹ Yuya Tsukimoto,¹
Yasuhiro Arikawa,¹ Masayoshi Onishi,¹ Shoji Ishizaka,² and Noboru Kitamura²

¹Department of Applied Chemistry, Faculty of Engineering, Nagasaki University, Bunkyo-machi, Nagasaki 852-8521

²Division of Chemistry, Graduate School of Science, Hokkaido University, Kita-ku, Sapporo 060-0810

Received July 23, 2010; E-mail: kumks@nagasaki-u.ac.jp

The pyrazolato (pz)- and 3,5-dimethylpyrazolato (Me₂pz)-bridged dinuclear platinum(II) and palladium(II) complexes of 2,2'-bipyrimidine (bpym), [Pt₂(bpym)₂(μ-pz')₂](PF₆)₂ (pz' = pz (**1a**) and Me₂pz (**1b**)) and [Pd₂(bpym)₂(μ-pz')₂](PF₆)₂ (pz' = pz (**2a**) and Me₂pz (**2b**)), have been synthesized and structurally characterized. The Pd–Pt complex, [PdPt(bpym)₂(μ-Me₂pz)₂](PF₆)₂ (**4b**), has also been synthesized and characterized by ¹H NMR spectroscopy. Among these Pt₂, Pd₂, and PdPt complexes, only **1a** and **1b** exhibit greenish blue and yellow-green luminescence, respectively, in the solid state at ambient temperature. The emissions of **1a** and **1b** in the solid state are tentatively assigned as the emission from the ³LC/MLCT and ³MMLCT excited states, respectively.

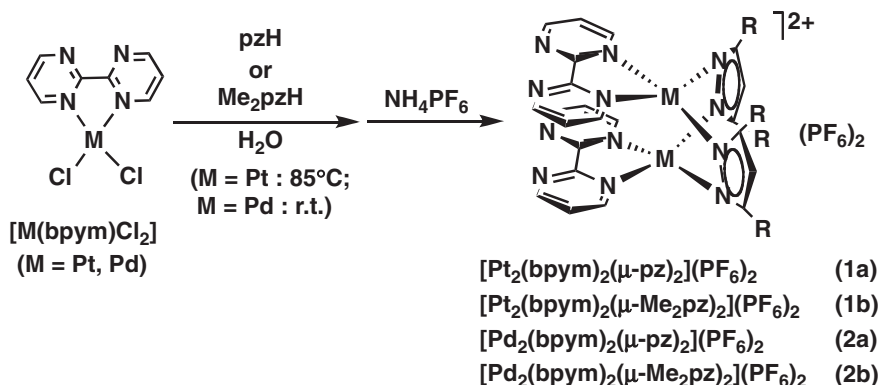
Platinum(II) complexes containing α-diimine, terpyridine, acetylide, or related ligands have attracted much attention in view of their luminescent properties and potential application to materials.^{1–17} Remarkable features of these complexes are that metal–metal interactions are expected in the solid state and in concentrated solutions. Furthermore the intramolecular metal–metal interactions between (π-type ligand)platinum units are also expected by constructing dinuclear complexes with face-to-face association of coordination planes. Their emissive states are attributed to a variety of low energy excited states depending on the nature of π-type ligands and the extent of intermolecular metal–metal interactions.

We have recently found that the heteropolynuclear complex of 3,5-dimethylpyrazolate, [Pt₂Ag₄(Me₂pz)₈] (Me₂pzH: 3,5-dimethylpyrazole) exhibits cluster-centered bright sky-blue luminescence and the emission energy can be controlled by the change of incorporated group 11 elements.^{18,19} Our preliminary examination of the luminescent properties of Pd analog, [Pd₂Ag₄(Me₂pz)₈], revealed that the Pd₂Ag₄ complex exhibits orange luminescence, indicating that the replacement of Pt atoms by Pd atoms results in the decrease of emission energy of Pd₂Ag₄ complex. It is thus interesting to compare luminescent properties of Pt₂, Pd₂, and PdPt complexes containing α-diimine ligands, though Pd₂ and PdPt complexes did not show luminescence at least at an ambient temperature. Herein we report the syntheses, structures, and luminescent properties of pyrazolato- and 3,5-dimethylpyrazolato-bridged dinuclear platinum(II), palladium(II), and their mixed-metal complexes of 2,2'-bipyrimidine.

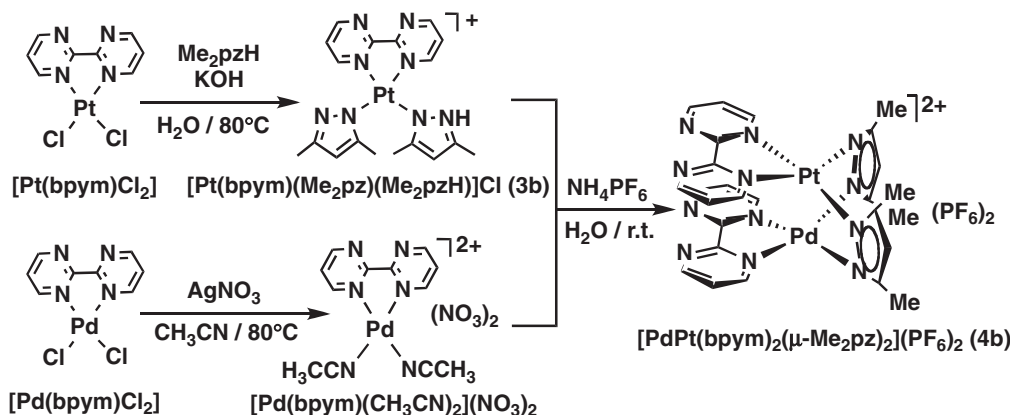
Results and Discussion

Synthesis and Characterization. The reaction of [Pt(bpym)Cl₂] (bpym: 2,2'-bipyrimidine) with pyrazole (pzH) and 3,5-

dimethylpyrazole (Me₂pzH) in a 1:1 ratio at 85 °C in water and an addition of NH₄PF₆ into the solution afforded pyrazolato-bridged dinuclear platinum(II) complexes, [Pt₂(bpym)₂(μ-pz)₂](PF₆)₂ (**1a**) and [Pt₂(bpym)₂(μ-Me₂pz)₂](PF₆)₂ (**1b**), respectively. The palladium analogs, [Pd₂(bpym)₂(μ-pz)₂](PF₆)₂ (**2a**) and [Pd₂(bpym)₂(μ-Me₂pz)₂](PF₆)₂ (**2b**), were obtained similarly by the reaction of [Pd(bpym)Cl₂] with pzH or Me₂pzH at an ambient temperature (Scheme 1). The ¹H NMR spectra of **2a** and **2b** closely resemble those of **1a** and **1b**, respectively, and the signals of **2a** and **2b** appear in higher field than those of **1a** and **1b** (Table 1). As is described below, **1a** and **1b** exhibit greenish blue and yellow-green luminescence, respectively, in the solid state at an ambient temperature upon exposure to UV radiation. However, the palladium analogs, **2a** and **2b**, do not exhibit luminescence at ambient temperature even in the solid state. It is thus interesting to study the luminescent properties of the mixed-metal complex, which contains both of Pt(II) and Pd(II) ions in the molecule. Because Pt(II) ion is more inert than Pd(II) ion, we adopted a strategy that the bridging ligands were introduced to [Pt^{II}(bpym)] unit first and then Pd(II) ion was reacted with the precursor. Namely [Pt(bpym)Cl₂] was reacted with Me₂pzH (2 equiv) in the presence of KOH to give a mononuclear complex, [Pt(bpym)(Me₂pz)(Me₂pzH)]Cl (**3b**). The reaction of **3b** with [Pd(bpym)(CH₃CN)₂](NO₃)₂, which was prepared by the reaction of [Pd(bpym)Cl₂] with AgNO₃, and an addition of NH₄PF₆ afforded a mixed-metal complex, [PdPt(bpym)₂(μ-Me₂pz)₂](PF₆)₂ (**4b**) (Scheme 2). The ¹H NMR spectrum of **4b** is shown in Figure 1 with those of **1b** and **2b**. Numerical data are also summarized in Table 1. The ¹H NMR spectrum of **4b** is very similar to the superposition of NMR spectra of **1b** and **2b** in the range of 9.5–7.5 ppm. However, **4b** exhibits only one H4 resonance of Me₂pz ligand at 6.18 ppm, which has different



Scheme 1. Preparative methods for $[\text{M}_2(\text{bpy})_2(\mu\text{-pz})_2](\text{PF}_6)_2$ ($M = \text{Pt}$ and Pd) and $[\text{M}_2(\text{bpy})_2(\mu\text{-Me}_2\text{pz})_2](\text{PF}_6)_2$ ($M = \text{Pt}$ and Pd).



Scheme 2. Preparative methods for $[\text{PdPt}(\text{bpy})_2(\mu\text{-Me}_2\text{pz})_2](\text{PF}_6)_2$ (**4b**).

Table 1. ^1H NMR Data in CD_3CN (δ)

	1a	1b	2a	2b	3b ^{a)}	4b
H6_{bpy}	9.35	9.30	9.29	9.26	9.33	9.32 (Pt site) 9.25 (Pd site)
H4_{bpy}	8.68	8.57	8.41	8.30	9.23	8.57 (Pt site) 8.30 (Pd site)
H5_{bpy}	7.85	7.80	7.81	7.77	7.68	7.81 (Pt site) 7.77 (Pd site)
H3_{pz} and H5_{pz}	7.85		7.78			
H4_{pz}	6.65		6.58			
$\text{H4}_{\text{Me}_2\text{pz}}$		6.24		6.10	5.75	6.18
CH_3		2.35		2.38	2.35, 1.65	2.41, 2.35

a) Measured in CDCl_3 .

chemical shift from those of **1b** and **2b**. This fact clearly indicates that **4b** is the mixed-metal complex of Pt and Pd and is not a mixture of **1b** and **2b**. Actually the ^1H NMR spectrum of the mixture of **1b** and **2b** exhibits two H4 resonances of Me_2pz ligand at 6.24 and 6.10 ppm (Figure S1).

We have not succeeded in obtaining single crystals suitable for the X-ray structural analysis of **4b**. However, it is obvious from the ^1H NMR spectrum that the complex cation of **4b** has C_s symmetry, because only single H4 resonance of Me_2pz ligands, a set of single H4, H5, and H6 resonances for $\text{Pt}(\text{bpy})$ unit and also a set of single H4, H5, and H6 resonances for $\text{Pd}(\text{bpy})$ unit were observed. These observa-

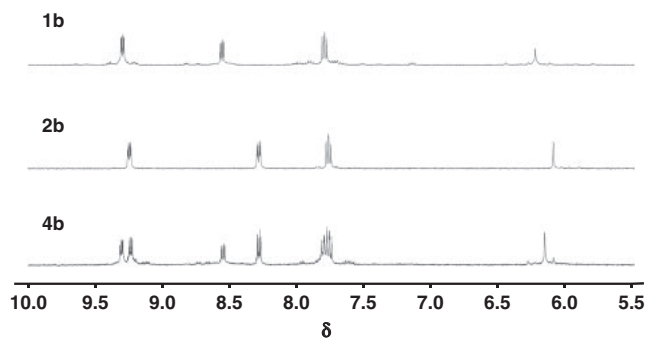


Figure 1. ^1H NMR spectra of $[\text{Pt}_2(\text{bpy})_2(\mu\text{-Me}_2\text{pz})_2](\text{PF}_6)_2$ (**1b**), $[\text{Pd}_2(\text{bpy})_2(\mu\text{-Me}_2\text{pz})_2](\text{PF}_6)_2$ (**2b**), and $[\text{PdPt}(\text{bpy})_2(\mu\text{-Me}_2\text{pz})_2](\text{PF}_6)_2$ (**4b**) in CD_3CN .

tions indicate that the structure of **4b** in solution is similar to that of **1b** and **2b**. Unfortunately **4b** does not exhibit luminescent properties in the solid state at ambient temperature upon exposure to UV radiation.

Crystal Structures. X-ray structural analyses of **1a**, **1b**, **2a**, and **2b** were performed (Table 2). The structure of the complex cation of **1a** is shown in Figure 2. Two $\text{Pt}(\text{bpy})$ units are bridged by two pyrazolate anions with face-to-face association of the coordination planes. The $\text{Pt}\cdots\text{Pt}$ distance in **1a** is $3.3589(5)\text{ \AA}$, and the tilt angle between adjacent platinum coordination planes defined by the four donor atoms, respectively, is $86(1)^\circ$ (Table 3). The $\text{Pt}\cdots\text{Pt}$ distance and the tilt angle

Table 2. Crystallographic Data for [Pt₂(bpym)₂(μ-pz)₂](PF₆)₂ (**1a**), [Pt₂(bpym)₂(μ-Me₂pz)₂](PF₆)₂ (**1b**), [Pd₂(bpym)₂(μ-pz)₂](PF₆)₂ (**2a**), and [Pd₂(bpym)₂(μ-Me₂pz)₂](PF₆)₂ (**2b**)

	1a	1b	2a	2b
Empirical formula	C ₂₂ H ₁₈ F ₁₂ N ₁₂ P ₂ Pt ₂	C ₂₆ H ₂₆ F ₁₂ N ₁₂ P ₂ Pt ₂	C ₂₂ H ₁₈ F ₁₂ N ₁₂ P ₂ Pd ₂	C ₂₆ H ₂₆ F ₁₂ N ₁₂ P ₂ Pd ₂
Formula weight	1130.57	1186.68	953.19	1009.30
<i>T</i> /K	296	296	296	296
<i>λ</i> /Å	0.71070	0.71070	0.71070	0.71070
Crystal system	orthorhombic	orthorhombic	orthorhombic	orthorhombic
Space group (No.)	<i>Pca</i> 2 ₁ (29)	<i>Pbca</i> (61)	<i>Pna</i> 2 ₁ (33)	<i>Pbca</i> (61)
<i>a</i> /Å	17.7518(5)	16.8152(9)	21.527(1)	16.4988(5)
<i>b</i> /Å	14.2988(4)	14.9288(7)	11.0681(8)	14.9573(5)
<i>c</i> /Å	12.7530(4)	29.996(2)	13.1289(5)	30.661(1)
<i>V</i> /Å ³	3237.1(3)	7529(1)	3128.1(5)	7566.3(7)
<i>Z</i>	4	8	4	8
ρ_{calcd} /g cm ⁻³	2.320	2.093	2.024	1.772
Crystal size/mm ³	0.50 × 0.30 × 0.15	0.20 × 0.20 × 0.20	0.70 × 0.10 × 0.04	0.60 × 0.40 × 0.40
2 θ_{max} /°	55.0	55.0	55.0	55.0
μ (Mo K α)/mm ⁻¹	8.805	7.576	1.364	1.133
Reflections collected	25259	58942	24545	57460
No. of unique reflections	3877 (<i>R</i> _{int} = 0.022)	8581 (<i>R</i> _{int} = 0.062)	3728 (<i>R</i> _{int} = 0.028)	8605 (<i>R</i> _{int} = 0.021)
Data/restraints/parameters	3877/0/422	8581/0/487	3728/0/452	5356/0/487
Final <i>R</i> indices	<i>R</i> ^a) = 0.028 [<i>I</i> > 2 σ (<i>I</i>)]	<i>R</i> = 0.047 [<i>I</i> > 2 σ (<i>I</i>)]	<i>R</i> = 0.050 [<i>I</i> > 2 σ (<i>I</i>)]	<i>R</i> = 0.058 [<i>I</i> > 3 σ (<i>I</i>)]
<i>R</i> indices	<i>R</i> ^b) = 0.052, <i>R</i> _w ^c) = 0.071	<i>R</i> = 0.085, <i>R</i> _w = 0.147	<i>R</i> = 0.069, <i>R</i> _w = 0.121	<i>R</i> = 0.105, <i>R</i> _w = 0.174
Goodness-of-fit on <i>F</i> ²	0.95	0.91	1.22	1.50
Largest diffraction peak/hole/eÅ ⁻³	0.99/−0.69	1.54/−1.38	1.48/−0.63	1.44/−0.80

a) $R1 = \sum ||F_o| - |F_c|| / \sum |F_o|$. b) $R = \sum (F_o^2 - F_c^2) / \sum F_o^2$. c) $R_w = [\sum [w(F_o^2 - F_c^2)^2] / \sum [w(F_o^2)^2]]^{1/2}$.

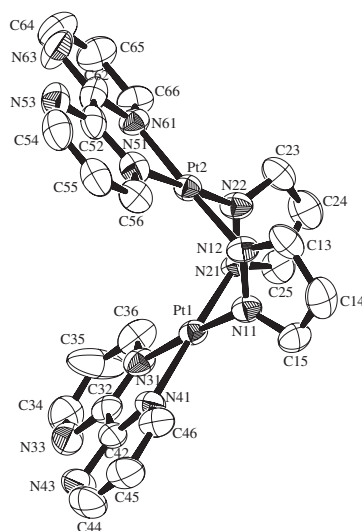
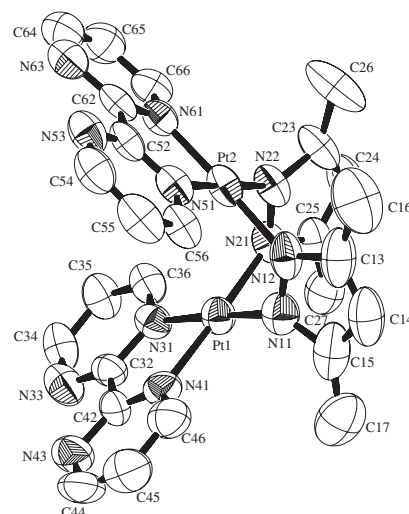
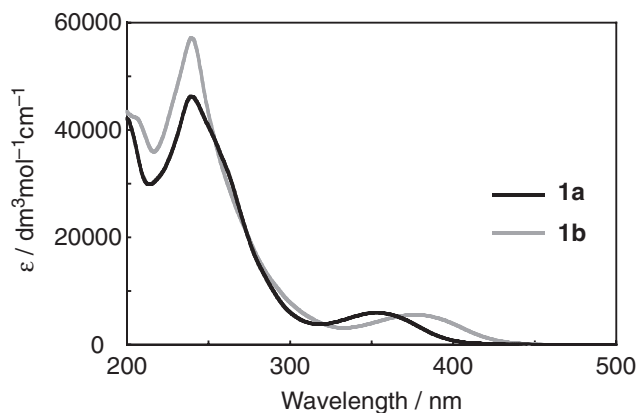


Table 3. Selected Bond Distances (Å) and Bond Angles (°) for **1a**, **1b**, **2a**, and **2b**

1a			
Pt1...Pt2	3.3589(5)		
Pt1–N11	2.013(10)	Pt2–N12	2.00(1)
Pt1–N21	1.987(8)	Pt2–N22	1.982(8)
Pt1–N31	2.026(10)	Pt2–N51	2.019(8)
Pt1–N41	2.021(9)	Pt2–N61	1.998(10)
N11–Pt1–N21	85.4(4)	N12–Pt2–N22	85.3(4)
N11–Pt1–N31	176.3(4)	N12–Pt2–N51	97.3(4)
N11–Pt1–N41	96.4(4)	N12–Pt2–N61	176.3(4)
N21–Pt1–N31	97.9(4)	N22–Pt2–N51	177.2(5)
N21–Pt1–N41	177.4(4)	N22–Pt2–N61	97.1(4)
N31–Pt1–N41	80.2(4)	N51–Pt2–N61	80.5(4)
1b			
Pt1...Pt2	3.1968(7)		
Pt1–N11	1.98(1)	Pt2–N12	1.99(1)
Pt1–N21	2.003(9)	Pt2–N22	1.997(10)
Pt1–N31	2.009(9)	Pt2–N51	2.000(9)
Pt1–N41	2.016(9)	Pt2–N61	1.985(10)
N11–Pt1–N21	86.6(4)	N12–Pt2–N22	85.0(4)
N11–Pt1–N31	177.3(4)	N12–Pt2–N51	96.6(4)
N11–Pt1–N41	97.0(4)	N12–Pt2–N61	177.1(4)
N21–Pt1–N31	96.1(4)	N22–Pt2–N51	178.0(4)
N21–Pt1–N41	176.4(4)	N22–Pt2–N61	97.5(4)
N31–Pt1–N41	80.3(4)	N51–Pt2–N61	80.9(4)
2a			
Pd1...Pd2	3.3337(9)		
Pd1–N11	2.015(9)	Pd2–N12	2.00(1)
Pd1–N21	2.000(8)	Pd2–N22	2.010(7)
Pd1–N31	2.026(9)	Pd2–N51	2.032(8)
Pd1–N41	2.044(7)	Pd2–N61	2.020(10)
N11–Pd1–N21	86.6(3)	N12–Pd2–N22	86.6(3)
N11–Pd1–N31	177.5(4)	N12–Pd2–N51	95.5(4)
N11–Pd1–N41	96.9(3)	N12–Pd2–N61	176.8(3)
N21–Pd1–N31	95.6(4)	N22–Pd2–N51	177.5(3)
N21–Pd1–N41	176.1(4)	N22–Pd2–N61	96.4(3)
N31–Pd1–N41	80.9(4)	N51–Pd2–N61	81.6(4)
2b			
Pd1...Pd2	3.1966(8)		
Pd1–N11	2.007(7)	Pd2–N12	1.971(8)
Pd1–N21	2.002(6)	Pd2–N22	1.987(6)
Pd1–N31	2.018(6)	Pd2–N51	1.998(6)
Pd1–N41	2.013(6)	Pd2–N61	1.998(7)
N11–Pd1–N21	87.1(3)	N12–Pd2–N22	85.7(3)
N11–Pd1–N31	177.2(2)	N12–Pd2–N51	95.3(3)
N11–Pd1–N41	97.3(3)	N12–Pd2–N61	176.0(3)
N21–Pd1–N31	95.3(2)	N22–Pd2–N51	178.0(2)
N21–Pd1–N41	175.6(3)	N22–Pd2–N61	98.1(3)
N31–Pd1–N41	80.3(2)	N51–Pd2–N61	80.8(3)

spectrum of [Pt(bpy)(Me₂pzH)₂](PF₆)₂ (Figure S4). The failure of the synthesis of [Pt(bpy)(pzH)₂](PF₆)₂, however, prevents us from unambiguous assignment of the absorption bands at 353 nm in **1a**. Thus we tentatively assigned the lowest

**Figure 3.** Perspective drawing of the complex cation of [Pt₂(bpy)₂(μ-Me₂pz)₂](PF₆)₂ (**1b**) with the atomic labeling scheme (50% probability ellipsoids).**Figure 4.** Electronic absorption spectra of **1a** (—) and **1b** (---) in CH₃CN at 298 K.

energy bands in **1b** at 377 nm as metal–metal-to-ligand charge transfer (MMLCT) transition. The systematic shift of the lowest energy absorption bands to lower energy was also observed for series of cyclometalated platinum(II) complexes, [Pt₂(C[^]N)₂(μ-pz')₂] (pz' = pz, Me₂pz, Me'Bupz, and 'Bu₂pz; Me'Bupz: 3-methyl-5-*tert*-butylpyrazolate, 'Bu₂pz: 3,5-bis(*tert*-butyl)pyrazolate),⁸ and [Pt₂(ppy)₂(μ-pz')₂] (pz' = pz, Ph₂pz, and 'Bu₂pz; Ph₂pz: 3,5-diphenylpyrazolate),²² with increase of the bulkiness of substituent groups on the pyrazolate ligands. The lowest energy absorption bands absent in the absorption spectrum of related mononuclear complex are assigned to MMLCT transition for [Pt₂(C[^]N)₂(μ-pz')₂].⁸ It is noteworthy that the MMLCT transitions are not observed explicitly for the cyclometalated platinum(II) complexes with pyrazolate and dimethylpyrazolate bridging ligands, [Pt₂(C[^]N)₂(μ-pz')₂] (pz' = pz and Me₂pz),⁸ [Pt₂(ppy)₂(μ-pz)₂],²² and [Pt₂(fppz)₂(μ-pz')₂] (fppz: 3-trifluoromethyl-5-(2-pyridyl)pyrazolate; pz' = pz and Me₂pz).²³

The pz-bridged complex, **1a**, exhibits an emission spectrum with distinct vibronic features in the solid state (λ_{max} =

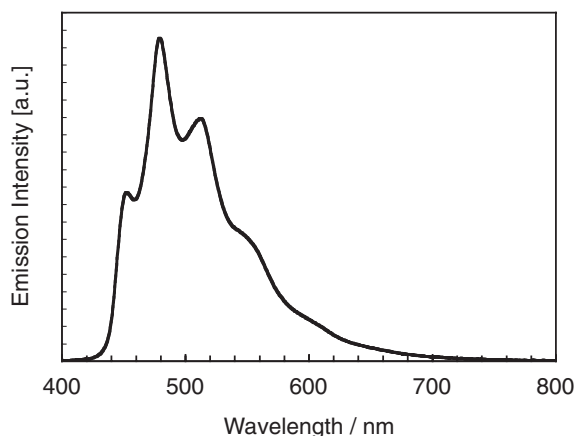


Figure 5. Emission spectra of $[\text{Pt}_2(\text{bpy})_2(\mu\text{-pz})_2](\text{PF}_6)_2$ (**1a**) in the solid state at 295 K ($\lambda_{\text{ex}} = 355$ nm).

Table 4. Emission Properties of $[\text{Pt}_2(\text{bpy})_2(\mu\text{-pz})_2](\text{PF}_6)_2$ (**1a**)^a and $[\text{Pt}_2(\text{bpy})_2(\mu\text{-Me}_2\text{pz})_2](\text{PF}_6)_2$ (**1b**)

	Crystal			In CH_3CN		
	$\lambda_{\text{max}}/\text{nm}$	$\tau/\mu\text{s}$	Φ	$\lambda_{\text{max}}/\text{nm}$	$\tau/\mu\text{s}$	Φ
1a	479	$\tau_1, 0.47; A_1, 0.38$ $\tau_2, 1.5; A_2, 0.62$	0.03	—	—	—
1b	536	0.0872	0.01	451	0.0047	0.0005

a) Emission decay curve was analyzed by the equation $I(t) = A_1 \exp(-t/\tau_1) + A_2 \exp(-t/\tau_2)$ using the nonlinear least-squares method.

479 nm, Figure 5). The vibronic peaks spaced by ca. 1300 cm^{-1} indicate that this transition is coupled to aromatic ring-breathing modes. The close similarity of the emission of **1a** in the solid state to those of $[\text{Pt}_2(\text{C}^{\wedge}\text{N})_2(\mu\text{-pz}')_2]$ and $[\text{Pt}_2(\text{fppz})_2(\mu\text{-pz}')_2]$ ($\text{pz}' = \text{pz}$ and Me_2pz) in the solid state as well as in frozen solution at 77 K indicates that the emissions of **1a** can also be assigned to the transition from the mixture of ligand-centered $\pi\text{-}\pi^*$ excited state and the metal-to-ligand charge transfer excited state ($^3\text{LC/MLCT}$).^{8,23–25} The observed luminescent lifetime for **1a** is in the microsecond regime, indicating that the emission is phosphorescence (Table 4). Although $[\text{Pt}_2(\text{ppy})_2(\mu\text{-pz})_2]$ exhibits distinct emission from $^3\text{LC/MLCT}$ state in 2-methyltetrahydrofuran (2-MeTHF) solution even at 295 K, **1a** does not exhibit emission in CH_3CN solution at room temperature. Details of the photophysical properties including suppression of the emission in CH_3CN solution have been theoretically investigated and they are discussed elsewhere.²⁵

The Me_2pz -bridged complex, **1b**, displays broad featureless emission spectra both in the solid state ($\lambda_{\text{max}} = 536$ nm) and in CH_3CN solution ($\lambda_{\text{max}} = 451$ nm) (Figure 6). The observed lifetime ($\tau = 0.0872\text{ }\mu\text{s}$) of the emission in the solid state for **1b** is shorter than that for **1a**. The change of the emissive states from $^3\text{LC/MLCT}$ excited state to $^3\text{MMLCT}$ excited state is observed for the cyclometalated Pt(II) complexes, $[\text{Pt}_2(\text{C}^{\wedge}\text{N})_2(\mu\text{-pz}')_2]$ ($\text{pz}' = \text{pz}$, Me_2pz , Me^tBupz , and $^t\text{Bu}_2\text{pz}$)^{8,24} and $[\text{Pt}_2(\text{ppy})_2(\mu\text{-pz}')_2]$ ($\text{pz}' = \text{pz}$, Ph_2pz , and $^t\text{Bu}_2\text{pz}$)²² with decrease of Pt–Pt distances. The driving force for the change of emissive states is attributed to the steric influence of bulkier

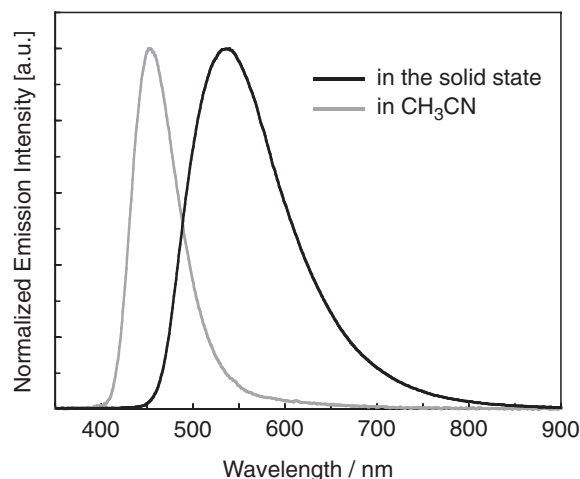


Figure 6. Normalized emission spectra of $[\text{Pt}_2(\text{bpy})_2(\mu\text{-Me}_2\text{pz})_2](\text{PF}_6)_2$ (**1b**) in the solid state (—) and in CH_3CN (—) at 295 K ($\lambda_{\text{ex}} = 355$ nm).

substituent groups on pyrazolate rings. Thus we tentatively assigned the emission of **1b** in the solid state as well as in CH_3CN solution as the emission from the $^3\text{MMLCT}$ excited state. It is interesting that the emissive state of **1b** ($^3\text{MMLCT}$) is different from that of $[\text{Pt}_2(\text{C}^{\wedge}\text{N})_2(\mu\text{-Me}_2\text{pz})_2]$ ($^3\text{LC/MLCT}$) in the solid state in spite of their similar Pt–Pt distances (**1b**, $3.1968(7)\text{ }\text{\AA}$; $[\text{Pt}_2(\text{C}^{\wedge}\text{N})_2(\mu\text{-Me}_2\text{pz})_2]$, $3.1914(9)\text{ }\text{\AA}$),⁸ though the emission of $[\text{Pt}_2(\text{C}^{\wedge}\text{N})_2(\mu\text{-Me}_2\text{pz})_2]$ in fluid solution at room temperature was assigned as the emission from the $^3\text{MMLCT}$ excited state.²⁴

Conclusion

The pyrazolato- and dimethylpyrazolato-bridged Pt_2 , Pd_2 , and PdPt complexes of bipyrimidine have been synthesized and characterized. The photophysical measurement of these complexes revealed that only Pt_2 complexes, **1a** and **1b**, exhibit luminescent properties at room temperature. The pz -bridged complex, **1a**, exhibits an emission spectrum with distinct vibronic features in the solid state. The emission was tentatively assigned as the emission from the mixture of ligand-centered $\pi\text{-}\pi^*$ excited state and the metal-to-ligand charge-transfer excited state ($^3\text{LC/MLCT}$). On the other hand, the Me_2pz -bridged complex, **1b**, displays broad featureless emission spectra both in the solid state and in CH_3CN solution. The emission of **1b** may be assigned as the emission from the $^3\text{MMLCT}$ excited state. The dependence of the emissive state on the Pt–Pt distance was observed for **1a** and **1b**. The Pt–Pt interaction in **1b** is strong enough to produce MMLCT photoluminescence in the solid state.

Experimental

Materials and Instrumentation. $[\text{Pt}(\text{bpy})\text{Cl}_2]$ ^{26,27} and $[\text{Pd}(\text{bpy})\text{Cl}_2]$ ^{28,29} were prepared by the reaction of $[\text{Pt}(\text{C}_2\text{H}_5\text{CN})_2\text{Cl}_2]$ ³⁰ and $[\text{Pd}(\text{CH}_3\text{CN})_2\text{Cl}_2]$ ³¹ with 2,2'-bipyrimidine, respectively, in acetonitrile. All other commercially available reagents were used as purchased. UV–vis spectra were recorded on a Hitachi U-3300 spectrophotometer at 20 °C. The ^1H NMR spectra were obtained at 300 MHz with a Varian Gemini 300 spectrometer.

Preparation of Complexes. **[Pt₂(bpym)₂(μ-pz)₂](PF₆)₂ (**1a**):** [Pt(bpym)Cl₂] (86 mg, 0.20 mmol) and pzH (16 mg, 0.23 mmol) were suspended in water (10 mL), and the mixture was stirred for 24 h at 85 °C under air. The red suspension was filtered, and NH₄PF₆ (65 mg, 0.40 mmol) was added to the filtrate to give red-orange precipitate. The solid was filtered, washed with water and diethyl ether, and dried in vacuo. Yield 90 mg (80%). It was recrystallized from CH₃CN/acetone/CH₂Cl₂ to give crystals suitable for X-ray structural analysis. Anal. Found: C, 23.41; H, 1.45; N, 14.71%. Calcd for C₂₂H₁₈F₁₂N₁₂P₂Pt₂: C, 23.37; H, 1.60; N, 14.87%. ¹H NMR (CD₃CN): δ 9.35 (dd, 4H, H₆_{bpym}, *J* = 1.9, 4.9 Hz), 8.68 (dd, 4H, H₄_{bpym}, *J* = 1.9, 5.8 Hz), 7.85 (m, 8H, (H₃_{pz}, H₅_{pz}, H₅_{bpym})), 6.65 (t, 2H, H₄_{pz}, *J* = 2.5 Hz).

[Pt₂(bpym)₂(μ-Me₂pz)₂](PF₆)₂ (1b**):** [Pt(bpym)Cl₂] (86 mg, 0.20 mmol) and Me₂pzH (19 mg, 0.20 mmol) were suspended in water (10 mL), and the mixture was stirred for 48 h at 85 °C under air. The red suspension was filtered, and NH₄PF₆ (65 mg, 0.40 mmol) was added to the filtrate to give red-orange precipitate. The solid was filtered, washed with water and diethyl ether, and dried in vacuo. Yield 71 mg (59%). It was recrystallized from CH₃CN/acetone/CH₂Cl₂ to give crystals suitable for X-ray structural analysis. Anal. Found: C, 25.91; H, 2.34; N, 13.78%. Calcd for C₂₆H₂₆F₁₂N₁₂P₂Pt₂: C, 26.32; H, 2.21; N, 14.16%. ¹H NMR (CD₃CN): δ 9.30 (dd, 4H, H₆_{bpym}, *J* = 2.0, 4.9 Hz), 8.57 (dd, 4H, H₄_{bpym}, *J* = 2.0, 5.8 Hz), 7.80 (dd, 4H, H₅_{bpym}, *J* = 4.9, 5.8 Hz), 6.24 (s, 2H, H₄_{Me₂pz}), 2.35 (s, 12H, CH₃).

[Pd₂(bpym)₂(μ-pz)₂](PF₆)₂ (2a**):** [Pd(bpym)Cl₂] (28 mg, 0.08 mmol) and pzH (14 mg, 0.21 mmol) were suspended in water (8 mL), and the mixture was stirred for 4 h at ambient temperature under air. The yellow suspension turned to a yellow solution. The addition of NH₄PF₆ (92 mg, 0.57 mmol) to the solution resulted in white precipitate. The solid was filtered, washed with water, and dried in vacuo. Yield 23 mg (59%). It was recrystallized from CH₃CN/EtOH to give crystals suitable for X-ray structural analysis. Anal. Found: C, 27.67; H, 1.58; N, 17.61%. Calcd for C₂₂H₁₈F₁₂N₁₂P₂Pd₂: C, 27.72; H, 1.90; N, 17.63%. ¹H NMR (CD₃CN): δ 9.29 (dd, 4H, H₆_{bpym}, *J* = 2.0, 4.9 Hz), 8.41 (dd, 4H, H₄_{bpym}, *J* = 2.0, 5.8 Hz), 7.81 (dd, 4H, H₅_{bpym}, *J* = 4.9, 5.8 Hz), 7.78 (d, 4H, H₃_{pz} and H₅_{pz}, *J* = 2.4 Hz), 6.58 (t, 2H, H₄_{pz}, *J* = 2.4 Hz).

[Pd₂(bpym)₂(μ-Me₂pz)₂](PF₆)₂ (2b**):** [Pd(bpym)Cl₂] (22 mg, 0.06 mmol) and Me₂pzH (14 mg, 0.14 mmol) were suspended in water (8 mL), and the mixture was stirred for 3 h at ambient temperature under air. The yellow suspension turned to yellow solution. The addition of NH₄PF₆ (30 mg, 0.18 mmol) to the solution resulted in white precipitate. The solid was filtered, washed with water, and dried in vacuo. Yield 13 mg (43%). It was recrystallized from CH₃CN/EtOH to give crystals suitable for X-ray structural analysis. Anal. Found: C, 31.04; H, 2.81; N, 16.51%. Calcd for C₂₆H₂₆F₁₂N₁₂P₂Pd₂: C, 30.94; H, 2.60; N, 16.65%. ¹H NMR (CD₃CN): δ 9.26 (dd, 4H, H₆_{bpym}, *J* = 2.1, 4.9 Hz), 8.30 (dd, 4H, H₄_{bpym}, *J* = 2.0, 5.7 Hz), 7.77 (dd, 4H, H₅_{bpym}, *J* = 4.9, 5.7 Hz), 6.10 (s, 2H, H₄_{Me₂pz}), 2.38 (s, 12H, CH₃). FABMS: *m/z* 864.4 [M]⁺.

[Pt(bpym)(Me₂pz)(Me₂pzH)]Cl (3b**):** [Pt(bpym)Cl₂] (102 mg, 0.24 mmol) and Me₂pzH (52 mg, 0.54 mmol) were added to an aqueous solution (8 mL) of KOH (34 mg, 0.61 mmol), and

the mixture was stirred for 2 h at 80 °C under air. The red-orange precipitate was filtered, washed with ether, and dried in vacuo. Furthermore, the product dissolving in the reaction solution was also extracted three times with CH₂Cl₂ (10 mL). The orange solution was filtered and concentrated. The addition of *n*-hexane into the solution resulted in orange precipitate. The precipitate was washed with *n*-hexane and dried in vacuo. Total yield 71 mg (49%). Anal. Found: C, 36.20; H, 3.91; N, 18.43%. Calcd for C₁₈H₂₃ClN₈OPt (**3b**·H₂O): C, 36.16; H, 3.88; N, 18.74%. ¹H NMR (CDCl₃): δ 9.33 (dd, 2H, H₆_{bpym}, *J* = 2.2, 4.2 Hz), 9.23 (dd, 2H, H₄_{bpym}, *J* = 2.1, 4.8 Hz), 7.68 (dd, 2H, H₅_{bpym}, *J* = 4.8, 5.7 Hz), 5.75 (s, 2H, H₄_{Me₂pz}), 2.35 (s, 6H, CH₃), 1.65 (s, 6H, CH₃). FABMS: *m/z* 543.2 [M - HCl]⁺.

[PdPt(bpym)₂(μ-Me₂pz)₂](PF₆)₂ (4b**):** [Pd(bpym)Cl₂] (35 mg, 0.11 mmol) and AgNO₃ (38 mg, 0.22 mmol) were suspended in CH₃CN (10 mL), and the mixture was stirred for 4 h at 80 °C under air. The yellow suspension was filtered to remove white precipitate of AgCl, and the yellow filtrate was concentrated to dryness. The yellow solid was dissolved in water (5 mL), and to this aqueous solution was added an aqueous solution (10 mL) of **3b** (60 mg, 0.10 mmol). The mixture was stirred for 1 h at an ambient temperature, and filtered. An addition of an aqueous solution (3 mL) of NH₄PF₆ (61 mg, 0.38 mmol) into the filtrate resulted in yellow precipitate. It was filtered, washed with water, and dried in vacuo. Yield 60 mg (50%). Anal. Found: C, 28.73; H, 2.51; N, 15.49%. Calcd for C₂₆H₂₆F₁₂N₁₂P₂PdPt: C, 28.44; H, 2.39; N, 15.31%. ¹H NMR (CD₃CN): δ 9.32 (dd, 2H, H₆_{bpym}(Pt site), *J* = 2.0, 4.8 Hz), 9.25 (dd, 2H, H₆_{bpym}(Pd site), *J* = 2.0, 4.8 Hz), 8.57 (dd, 2H, H₄_{bpym}(Pt site), *J* = 2.0, 5.8 Hz), 8.30 (dd, 2H, H₄_{bpym}(Pd site), *J* = 2.0, 5.8 Hz), 7.81 (dd, 2H, H₅_{bpym}(Pt site), *J* = 4.9, 5.8 Hz), 7.77 (dd, 2H, H₅_{bpym}(Pd site), *J* = 4.9, 5.8 Hz), 6.18 (s, 2H, H₄_{Me₂pz}), 2.41 (s, 6H, CH₃), 2.35 (s, 6H, CH₃). FABMS: *m/z* 951.1 [M]⁺.

X-ray Crystallography. Crystals suitable for X-ray structural analyses were obtained by recrystallization as mentioned above. The crystals, **1a**, **1b**, **2a**, and **2b** were mounted on glass fibers. Intensity data were collected on a Rigaku/MSC Mercury CCD diffractometer using graphite-monochromated Mo Kα (*λ* = 0.71070 Å) radiation at 296 K. Final cell parameters were obtained from a least-squares analysis of reflections with *I* > 10σ(*I*). The data were corrected for Lorentz and polarization effects. An empirical absorption correction was applied.³²

The crystal structure of **1a** was solved by heavy-atom method by using DIRDIF94.³³ The positional and thermal parameters of non-H atoms were refined anisotropically except for the F atoms in one of the PF₆ ions (F21, F22, F23, F24, F25, and F26) by the full-matrix least-squares method, and those six F atoms were refined isotropically. The crystal structures of **1b**, **2a**, and **2b** were solved by direct method (SIR92).³⁴ The positional and thermal parameters of non-H atoms were refined anisotropically by the full-matrix least-squares method. The minimized function was Σw(*F*_o² - *F*_c²),² where *w*⁻¹ = σ²(*F*_o²) + (*p*(Max(*F*_o², 0) + 2*F*_c²)/3)² (*p* = 0.03 for **1a**, 0.05 for **1b** and **2a**, 0.09 for **2b**). Hydrogen atoms were included at calculated positions with fixed displacement parameters (1.2 times the displacement parameters of the host atom). In the final cycle of the refinement, parameter shifts were less than 0.1σ. No correction was made for secondary extinction.

All calculations were performed using teXsan.³⁵ Further crystallographic data are given in Table 2. Listings of the selected bond distances and angles are summarized in Table 3. Non-hydrogen atom coordinates, anisotropic thermal parameters, and full listings of bond distances and angles are provided as Supporting Information. Crystallographic data have been deposited with Cambridge Crystallographic Data Centre: Deposition number CCDC-776348–776351 for **1a**, **1b**, **2a**, and **2b**, respectively. Copies of the data can be obtained free of charge via <http://www.ccdc.cam.ac.uk/conts/retrieving.html> (or from the Cambridge Crystallographic Data Centre, 12, Union Road, Cambridge, CB2 1EZ, U.K.; Fax: +44 1223 336033; e-mail: deposit@ccdc.cam.ac.uk).

Photophysical Measurement. Corrected emission spectra were obtained by using a red-sensitive photodetector (Hamamatsu PMA-11, model C5966-23) and the third-harmonic generation of an Nd:YAG Laser (Continuum Surelite) at 355 nm excitation. The instrumental responses of the system were corrected by using a software package for the detector. Lifetime measurements were conducted by using a streak camera (Hamamatsu C4334) as a detector. Emission quantum yields were estimated by using an acetonitrile solution of [Ru(bpy)₃](PF₆)₂ ($\Phi_{\text{em}} = 0.061$) as a standard.³⁶ Sample solutions were deaerated thoroughly by purging with an Ar gas stream for 15 min prior to the experiments and then sealed in their cells. Emission quantum yields in the solid state were determined by using a Hamamatsu Photonic Absolute PL Quantum Yield Measurement System C9920-02.

This work was partially supported by a Grant-in-Aid for Scientific Research (No. 21550062).

Supporting Information

Additional characterization data (¹H NMR spectrum of a mixture of **1b** and **2b**, perspective drawing of the complex cation of **2a** and **2b**, absorption spectrum of [Pt(bpy)₂](Me₂pzh)₂(PF₆)₂, and emission decay curves of **1a** and **1b**). This material is available free of charge on the web at <http://www.csj.jp/journals/bcsj/>.

References

- S.-W. Lai, C.-M. Che, *Top. Curr. Chem.* **2004**, *241*, 27.
- F. N. Castellano, I. E. Pomestchenko, E. Shikhova, F. Hua, M. L. Muro, N. Rajapakse, *Coord. Chem. Rev.* **2006**, *250*, 1819.
- K. M.-C. Wong, V. W.-W. Yam, *Coord. Chem. Rev.* **2007**, *251*, 2477.
- M. Kato, *Bull. Chem. Soc. Jpn.* **2007**, *80*, 287.
- V. M. Miskowski, V. H. Houlding, *Inorg. Chem.* **1991**, *30*, 4446.
- J. A. Bailey, V. M. Miskowski, H. B. Gray, *Inorg. Chem.* **1993**, *32*, 369.
- W. B. Connick, V. M. Miskowski, V. H. Houlding, H. B. Gray, *Inorg. Chem.* **2000**, *39*, 2585.
- B. Ma, J. Li, P. I. Djurovich, M. Yousufuddin, R. Bau, M. E. Thompson, *J. Am. Chem. Soc.* **2005**, *127*, 28.
- S.-Y. Chang, J. Kavitha, S.-W. Li, C.-S. Hsu, Y. Chi, Y.-S. Yeh, P.-T. Chou, G.-H. Lee, A. J. Carty, Y.-T. Tao, C.-H. Chien, *Inorg. Chem.* **2006**, *45*, 137.
- E. Sakuda, A. Funahashi, N. Kitamura, *Inorg. Chem.* **2006**, *45*, 10670.
- S. Develay, O. Blackburn, A. L. Thompson, J. A. G. Williams, *Inorg. Chem.* **2008**, *47*, 11129.
- T. J. Wadas, Q.-M. Wang, Y.-j. Kim, C. Flaschenreim, T. N. Blanton, R. Eisenberg, *J. Am. Chem. Soc.* **2004**, *126*, 16841.
- S. C. F. Kui, S. S.-Y. Chui, C.-M. Che, N. Zhu, *J. Am. Chem. Soc.* **2006**, *128*, 8297.
- C.-K. Koo, B. Lam, S.-K. Leung, M. H.-W. Lam, W.-Y. Wong, *J. Am. Chem. Soc.* **2006**, *128*, 16434.
- Y. Sun, K. Ye, H. Zhang, J. Zhang, L. Zhao, B. Li, G. Yang, B. Yang, Y. Wang, S.-W. Lai, C.-M. Che, *Angew. Chem., Int. Ed.* **2006**, *45*, 5610.
- P. Wu, E. L.-M. Wong, D.-L. Ma, G. S.-M. Tong, K.-M. Ng, C.-M. Che, *Chem.—Eur. J.* **2009**, *15*, 3652.
- J. Ni, Y.-H. Wu, X. Zhang, B. Li, L.-Y. Zhang, Z.-N. Chen, *Inorg. Chem.* **2009**, *48*, 10202.
- K. Umakoshi, T. Kojima, K. Saito, S. Akatsu, M. Onishi, S. Ishizaka, N. Kitamura, Y. Nakao, S. Sakaki, Y. Ozawa, *Inorg. Chem.* **2008**, *47*, 5033.
- K. Umakoshi, K. Saito, Y. Arikawa, M. Onishi, S. Ishizaka, N. Kitamura, Y. Nakao, S. Sakaki, *Chem.—Eur. J.* **2009**, *15*, 4238.
- K. Sakai, T. Sato, T. Tsubomura, K. Matsumoto, *Acta Crystallogr., Sect. C* **1996**, *52*, 783.
- J. Pérez, A. Espinosa, J. M. Galiana, E. Pérez, J. L. Serrano, M. A. G. Aranda, M. Insausti, *Dalton Trans.* **2009**, 9625.
- A. A. Rachford, F. N. Castellano, *Inorg. Chem.* **2009**, *48*, 10865.
- S.-Y. Chang, J.-L. Chen, Y. Chi, Y.-M. Cheng, G.-H. Lee, C.-M. Jiang, P.-T. Chou, *Inorg. Chem.* **2007**, *46*, 11202.
- K. Saito, Y. Nakao, S. Sakaki, *Inorg. Chem.* **2008**, *47*, 4329.
- K. Saito, Y. Nakao, K. Umakoshi, S. Sakaki, *Inorg. Chem.* **2010**, *49*, 8977.
- P. M. Kiernan, A. Ludi, *J. Chem. Soc., Dalton Trans.* **1978**, 1127.
- W. Kaim, A. Dogan, M. Wanner, A. Klein, I. Tiritiris, T. Schleid, D. J. Stufkens, T. L. Snoeck, E. J. L. McInnes, J. Fiedler, S. Zálaiš, *Inorg. Chem.* **2002**, *41*, 4139.
- M. P. Garcia, J. L. Millan, M. A. Esteruelas, L. A. Oro, *Polyhedron* **1987**, *6*, 1427.
- Q. Jaradat, K. Barqawi, T. S. Akasheh, *Inorg. Chim. Acta* **1986**, *116*, 63.
- V. Y. U. Kukushkin, Å. Oskarsson, L. I. Elding, S. Jonasdottir, *Inorg. Synth.* **1997**, *31*, 279.
- F. L. Wimmer, S. Wimmer, P. Castan, R. J. Puddephatt, *Inorg. Synth.* **1992**, *29*, 185.
- R. A. Jacobson, *REQABS, Version 1.1*, Molecular Structure Corp., The Woodlands, TX, **1998**.
- P. T. Beurskens, G. Admiraal, G. Beurskens, W. P. Bosman, R. de Gelder, R. Israel, J. M. M. Smits, *The DIRDIF94 Program System*, Crystallography Laboratory, University of Nijmegen, The Netherlands, **1994**.
- A. Altomare, G. Casciarano, C. Giacovazzo, A. Guagliardi, M. C. Burla, G. Polidori, M. Camalli, *J. Appl. Cryst.* **1994**, *27*, 435.
- teXsan: *Crystal Structure Analysis Package*, Molecular Structure Corporation, The Woodlands, TX 77381, USA, **1999**.
- K. Kalyanasundaram, *Photochemistry of Polypyridine and Porphyrin Complexes*, Academic Press, London, **1992**.